Hindawi

Research Article

Multiobjective Optimization of WEDM Parameters on the Mg-HNT-Zr Hybrid Metal Matrix Composite Using Taguchi-Coupled GRA

A. Jayaganthan [ID],[1] **M. Manickam** [ID],[2] **S. Prathiban**,[3] **M. Amarnath** [ID],[4]
Karthikeyan Subramanian [ID],[5] **M. Babu** [ID],[6] **P. Dharmadurai** [ID],[7] **and Yesgat Adamassu** [ID][8]

[1]*Department of Automobile Engineering, Sathyabama Institute of Science and Technology, Chennai, Tamil Nadu 600119, India*
[2]*Department of Mechanical Engineering, Bharath Institute of Higher Education and Research, Chennai 600073, India*
[3]*Department of Mechanical Engineering, Annamalai University, Chidambaram, Tamil Nadu, India*
[4]*Department of Mechatronics Engineering, Sathyabama Institute of Science and Technology, Chennai, Tamil Nadu 600119, India*
[5]*Department of Mechanical Engineering, Dhanalakshmi Srinivasan College of Engineering and Technology, Chennai, Tamil Nadu, India*
[6]*Department of Mechanical Engineering, SRM Easwari Engineering College, Chennai, India*
[7]*Department of Aeronautical Engineering, Mahendra Engineering College, Namakkal, Tamil Nadu, India*
[8]*Defence University College, Bishoftu, Ethiopia*

Correspondence should be addressed to Yesgat Adamassu; yesgat.admassu@dec.edu.et

The current research deals with Taguchi-coupled grey relational analysis (GRA) multiobjective optimization of wire electric discharge machining (WEDM) for better surface roughness (Ra) and the material removal rate (MRR) over magnesium/halloysite nano tube/zirconium (Mg/HNT/Zr) metal matrix composite (MMC). Hybrid composites are created through the powder metallurgy route by varying the weight percentage of reinforcements HNT (5 and 10%) and Zr (0.5 and 1%) to the weight of the base material magnesium. Machining is carried out by varying the factors such as reinforcement's weight percentage, pulse OFF time, pulse ON time, and wire feed (WF) based on Taguchi's L27 orthogonal array. The response surface roughness (Ra) and the material removal rate (MRR) were studied through Taguchi-coupled GRA to evaluate the optimized machining parameters. ANOVA results reveal the percentage contribution of certain factors over the machining of composites. The developed regression model proved that the predicted values were merely similar to the experimental values of MRR and Ra. The best parametric combinations obtained from optimization are inline as the minimum weight percentage of reinforcements, and higher Pon, higher WF, and the lowered Poff are used to attain the best rate of MRR during machining and for minimized surface roughness.

1. Introduction

MMCs are excellent materials in which high-strength and hard refractory ceramics are reinforced with the ductile metal matrix. Aluminum, magnesium, copper, titanium, and zinc are the commonly used lightweight matrix material and carbides, nitrides, oxides, and borides are the commonly used reinforcements in the form of particulates, whiskers, or fibers [1]. Strong attention to the evolution of MMCs is due to the improved properties such as strength,

hardness, wear resistance, corrosion resistance, higher thermal, and electrical conductivities combined with significant weight-reducing over alloys. Due to these superior properties of MMCS, they are widely used in automotive, aerospace, construction, and marine industries [1]. Amongst the several matrix materials used in MMCs, aluminum and magnesium matrices are used as the most common materials due to their low density, less weight, good corrosion resistance, high electrical and thermal conductivity, and low cost [2].

The MMCs can be fabricated by the different techniques such as the selection of suitable processing techniques on matrix material, quantity, and the nature of reinforcements and application. Liquid state, vapor state, and solid-state processing are the three major types of composite fabrication methods widely used. The solid-state handling approach incorporates the creation of MMC in the strongest state itself without softening the components, which results in the holding of the lattice stage and the support stage by common dispersal taking place among them in strong positions at discernible temperature and are lower than the exceptional weight. The fundamental preferred position of this procedure is that the collection of metals that can be dealt with is progressively broad and the assistant handling is negligible. Powder metallurgy and diffusion bonding methods are the most commonly used methods to make solid-state processing [3].

Powder metallurgy involves powders for manufacturing metal in the metal matrix composite with the sequence of blending, compaction, and sintering. This technique involves three main processes as shown in Figure 1.

The reinforcement and matrix powders are combined to develop a homogenous mixture with the help of a ball milling or mechanical stirrer or magnetic stirrer or ultrasonicator, etc. Then, the mixed powders are cold-pressed in a die to make the mixtures turn into a solid green composite, and this process is called compaction. The final step is the sintering process; here, the green composite is kept in a furnace at below-melting temperature to make a full solid composite. Sometimes the compaction process is carried out at an increased temperature, which is called hot pressing. Powder metallurgy permits minimizing machining operation on account of forming parts with minimum tolerance. Powder metallurgy allows the development of materials, which cannot be made by using any other technologies such as hard materials, refractory materials, porous metals, wear-resistant materials, blends of dissimilar metals, permanent magnets, possessing various melting points or are insoluble in the molten state, and different combinations of metals with nonmetals [4].

Machining is one of the important aspects of manufacturing processes by which excess materials are constantly removed by trimming from a preformed object that takes place in the form of solid chips or metal powders to get the desired shape, finish, and tolerance. The materials cannot be commercialized into applications directly without machining, as a minimum machining process is needed to get the required shape [5]. Traditional and nontraditional machining are the two different ways of machining. The major hindrance in the growth of MMCs was that of machining by using traditional techniques due to the property of superior hardness and the presence of reinforcement. The use of customary machinery to machine hard composite materials causes severe tool wear owed to the rough nature of the reinforcement. At the same time, with their various sophisticated technologies and features, nonconventional machining methods, also known as noncontact metal removal methods, have gained a reputation for successfully machining MMCs in industries [6]. Nontraditional machining processes are used to machine MMCs including electrical discharge machining (EDM), abrasive jet
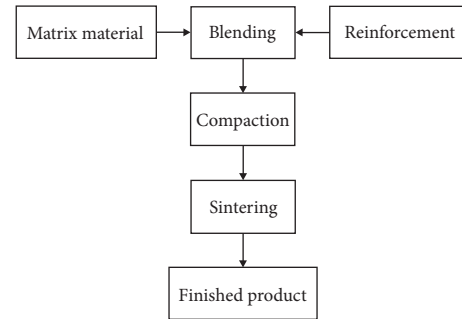
Figure 1: Powder metallurgy process.

machining (AJM), electrochemical machining (ECM), and laser beam machining (LBM). The wire electrical discharge machining (WEDM), a commonly accepted nontraditional machining technology for complicated precision components, discovered an effective metal removal approach for MMCs to enhance the cut quality at a specified cost. For a composite material that is made of different materials with different properties, the WEDM process is recommended for a more precise and accurate resulting surface finish.

WEDM is an unconventional machining process that is defined as a method in which materials are removed from the workpiece in a maximum accurate and effective manner [7]. WEDM is a high-precision cutting procedure that may be used on practically on any electrically conductive material. A thin, electrically charged wire usually made of a brass material gripped between the lower and upper mechanical guides constructs one electrode, while the material remaining cut forms another electrode. Electrical discharge between material and wire creates sparks that instantly cuts the excess material. Then, the debris are being flushed away by sinking the wire and workpiece in deionized water. Among the spoke explores broadly held in this field, just the sinking EDM process was commonly revealed, and significant on WEDM [8].

2. Materials and Methods

2.1. Materials. Hybridized Mg composites are often made by using the powder metallurgy (PM) process, which involves adding Zr and HNT particles to the basic material Mg in varying weight percentages. Aluminum and silica-rich double-layered aluminosilicate HNT were taken as a primary reinforcement for its ecofriendly, nontoxic, high strength, corrosion resistance, and wear-withstanding properties [9, 10]. HNT is a multiwalled kaolin clay with the structural formula $(H_4AL_2O_9Si_2.2H_2O)$ that was purchased from Sigma-Aldrich Company (USA).

Zr was selected as the reinforcing material for its wear resistance and high corrosion resistance properties such as high temperatures [11]. Zr compounds are used extensively in biomedical uses, including hip replacements, knee, and dental implants. It is also used in some prosthetic and therapeutic devices. As a result, Zr was chosen as a reinforcing material for hybrid biocompatible magnesium MMCs [1, 12].

2.2. *Composite Fabrication.* Powder metallurgy, which comprises the processes of sintering, compression, and blending, is the most efficient method of producing MMCs. Blending is one of the dynamic methods in PM, as the metallic powder particles are combined with reinforcing particles [13, 14]. The weight level of essential HNT fortification is fluctuated in the scope of 5 and 10, though the weight percent of optional Zr support is changed in the range of 0.5 and 1.0. In light of the writing review and starter trial examination results, the measure of reinforcements is fixed [15]. Nine distinctive magnesium MMCs were arranged by differing HNT and Zr percentages as specified in Table 1 alongside an unadulterated Mg sample.

The mixed powders were crushed under pressure in a die, then sintering was carried out in a hot furnace. Furthermore, as compared to the ingot metallurgical method, powder metallurgy has the ability to eliminate reinforcement separation. Figure 2 shows the powder metallurgy process for composite fabrication.

The blending process was performed by mixing the base material and reinforcement at a steady speed for 2 hours by using a magnetic stirrer. Figure 3 illustrates the SEM image of the base material and reinforcement's well-blended powder composition.

The sample was compressed using a hydraulic press machine with a 40 mm diameter die, a 560 Mpa load, and a 10-minute dwell time. Finally, under an argon gas atmosphere, the compressed green composite was sintered at 550°C in a muffle furnace, and sintered samples were then cooled down in the furnace [3]. Images of sintered composite material samples are displayed in Figure 2.

Density and hardness are the important physical property of the material corresponding to lightweight applications. The variation of density and microhardness for the unreinforced and as well as HNT and Zr reinforced in the various composition of composites is given in Table 1. Since the density of HNT (2.53 g/cm^3) and Zr (6.49) is higher than the matrix material Mg (1.738 g/cm^3), the addition of reinforcements leads to an increase in the density of the material. An increment in hardness with the increase in HNT and Zr weight rate might be ascribed to the higher hardness of support. Thus, both material phases with the great bonding illustrations have higher hardness.

2.3. *Machining Condition and Measurement.* Taguchi's DOE approach based on OA was used for designing the experiment by varying considerations at different levels. Minitab programming was utilized for this reason and the L27 symmetrical cluster was planned by using five factors that is the weight proportion of HNT and Zr over the pure Mg, pon, poff, and WF having three stages revealed in Table 2 were selected for this study in light of the writing review, specialists' recommendations, and preliminary trials. The response parameters were the material removal rate (MRR) and surface roughness (Ra). The appropriated experimental design obtained by using the L27 orthogonal array (OA)

chosen for the considered WEDM process parameters is shown in Table 3 and 4.

Surface roughness (Ra) and the material removal rate (MRR) are considered response parameters because the surface roughness value plays an important role in any newer material and likewise the MRR is also most important to commercialize the material economically. PCE-RT 1200 (the UK make) surface roughness tester was used to determine the roughness value over the surface of the machined composites for each trial. The parameter MRR during the WEDM process was determined by the following equation which incorporates the measure of material evacuated.

$$MRR = \frac{Wa - Wb}{t} \frac{g}{\min},$$ (1)

where Wa is the mass of workpiece material prior to machining, Wb is the mass of workpiece material in the wake of machining, and t is the duration of machining.

The machining process for the newly developed composites was carried out by using the EXETEKEX40 WEDM setup, as displayed in Figure 4. The machine had a brass wire of diameter 0.25 mm and the wire material was fed into the workpiece material so as to machine the surface with precise dimensions and all other relative fundamental machine specifications and other relevant general process parameters are provided in Table 4.

To know the deviation between test esteems and ideal cutting qualities, a quality misfortune capacity approach was prescribed by Taguchi. In the Taguchi strategy, the reaction factors were broken down as far as signal-to-noise (S/N) proportions, which records the affectability of yield estimated to the clamor factor or wild factor. The best possible S/N proportions figuring criteria must be picked from the three criteria in particular "larger is better," "nominal is better," and "smaller is better." The difference between measured data and the ideal value is expected to be as small as possible. The generic form of the S/N ratio then becomes small for surface roughness (Ra) so the equation can be described as follows:

$$n = -10 \log_{10} \left(\frac{1}{n} \sum_{i=1}^{n} yi^2 \right).$$ (2)

The difference between measured data and the ideal value is expected to be as large as possible. The generic form of S/N ratio then becomes maximum for the material removal rate (MRR) so the equation can be represented as follows:

$$n = -10 \log_{10} \left(\frac{1}{n} \sum_{i=1}^{n} \frac{1}{yi^2} \right).$$ (3)

ANOVA was performed to recognize the noteworthiness of every parameter over the reaction factors. Furthermore, the rate impact of each factor over the response variable was additionally distinguished from the ANOVA study by utilizing a consecutive aggregate of square values. And a p value of under 0.05 had a significant effect. Taguchi S/N proportions investigation was constrained to take care of just

TABLE 1: Results of hardness and density tests.

S. No	Composition	Hardness value for (100 gm.)	Density (g/cm^3)
1	Pure Mg	28.4	1.636
2	Mg-HNT 5%	34.8	1.638
3	Mg-HNT 10%	36.7	1.675
4	Mg-Zr 0.5%	32.7	1.619
5	Mg-Zr 1%	33.4	1.645
6	Mg-HNT 5%-Zr 0.5%	35.3	1.658
7	Mg-HNT 5%-Zr 1%	36.4	1.630
8	Mg-HNT 10%-Zr 0.5%	36.7	1.696
9	Mg-HNT 10%-Zr 1%	38.1	1.659
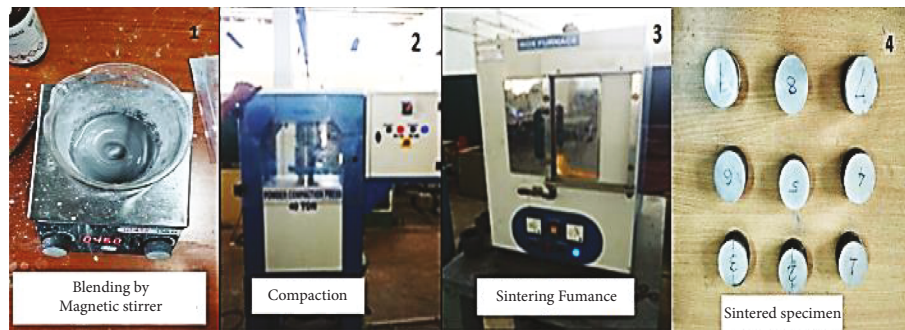
FIGURE 2: Composite development steps and prepared specimens.
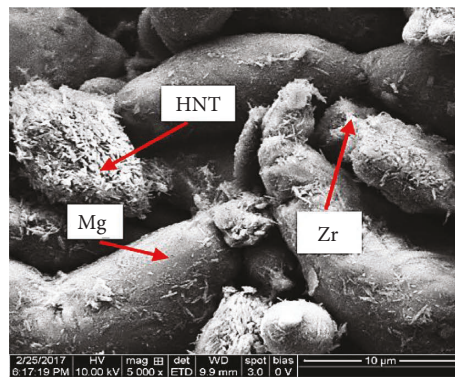
FIGURE 3: SEM micrograph of the well-mixed powder structure.

TABLE 2: Machining factors and levels (WEDM).

Factors	Codes	Level 1	Level 2	Level 3
HNT %	A	0	6	11
Zr %	B	0	0.6	1
Pulse on time (μs)	C	10	11	12
Pulse off time (μs)	D	15	16	17
Wire feed (m/min)	E	4	5	6

single-objective optimization issues. To advance the information parameters for multiobjective such as the material removal rate and surface roughness, a multiobjective streamlining named grey relational investigation with Taguchi configuration is a superior arrangement through GRA [16]. First, multiresponse parameters could be changed into a solitary target capacity, and afterwards, qualities of the ensuing ideal arrangement of parameters can be resolved.

TABLE 3: L27 experimental design with response variables.

Trial no.	HNT wt.%	Zr wt. %	P on	P off	Wire feed	MRR (g/min)	Ra (μm)	SNRA MRR	SNRA Ra
1	0	0	10	15	4	1.734	2.168	4.7809819	−6.7212
2	0	0	10	15	5	1.789	2.203	5.0522068	−6.8603
3	0	0	10	15	6	1.814	2.264	5.1727457	−7.0975
4	0	0.5	11	16	4	1.712	2.379	4.6700752	−7.5279
5	0	0.5	11	16	5	1.735	2.412	4.7859896	−7.6475
6	0	0.5	11	16	6	1.777	2.478	4.9937486	−7.882
7	0	1	12	17	4	1.695	2.454	4.5833941	−7.7975
8	0	1	12	17	5	1.715	2.496	4.6852825	−7.9449
9	0	1	12	17	6	1.732	2.597	4.7709578	−8.2894
10	5	0	11	17	4	1.603	2.452	4.0986704	−7.7904
11	5	0	11	17	5	1.639	2.497	4.2915791	−7.9484
12	5	0	11	17	6	1.698	2.532	4.5987537	−8.0693
13	5	0.5	12	15	4	1.664	3.053	4.4230664	−9.6945
14	5	0.5	12	15	5	1.69	3.126	4.5577341	−9.8998
15	5	0.5	12	15	6	1.703	3.197	4.624293	−10.095
16	5	1	10	16	4	1.498	2.788	3.5102363	−8.9059
17	5	1	10	16	5	1.513	2.867	3.5967786	−9.1486
18	5	1	10	16	6	1.542	2.947	3.7616875	−9.3876
19	10	0	12	16	4	1.659	2.769	4.3969277	−8.8465
20	10	0	12	16	5	1.684	2.815	4.5268417	−8.9896
21	10	0	12	16	6	1.692	2.874	4.5680072	−9.1697
22	10	0.5	10	17	4	1.412	2.489	2.9966939	−7.9205
23	10	0.5	10	17	5	1.498	2.543	3.5102363	−8.1069
24	10	0.5	10	17	6	1.545	2.612	3.7785697	−8.3395
25	10	1	11	15	4	1.568	3.102	3.9069212	−9.8328
26	10	1	11	15	5	1.594	3.178	4.0497663	−10.043
27	10	1	11	15	6	1.623	3.256	4.2063704	−10.254

FIGURE 4: Wire cut EDM machine setup.

TABLE 4: Key features of selected WEDM machine.

S. No.	Parameters of WEDM	Range/values
1.	Discharge current	10 A
2.	Gap voltage	20 V
3.	Pulse ON time	10–12 μs
4.	Pulse OFF time	15–17 μs
5.	Wire material	Cu
6.	Wire diameter	0.25 mm
7.	Wire feed (WF)	4–6 m/min
8.	Wire tension	8 N
9.	Workpiece height	30 mm
10.	Dielectric fluid	Deionized water

Furthermore, the Taguchi plan with grey relational analysis is a strong technique to take care of the multiobjective issues.

The primary stage is to standardize the deliberate yield work independently and it is fundamentally the same as the S/N proportions computation in the Taguchi strategy where various models are pursued. The "smaller is better" standardization condition was chosen for normalizing surface roughness and the corresponding formula can be represented as follows:

$$Y_{ij} = \frac{\left(\max(z_{ij}) - (zij)\right)}{\max(z_{ij}) - \min(z_{ij})}. \tag{4}$$

If there should arise an occurrence of MRR, the criteria picked for normalizing is "larger is better" and the equation is as follows:

$$Y_{ij} = \frac{\left(Z_{ij} - \min(z_{ij})\right)}{\max(z_{ij}) - \min(z_{ij})}, \tag{5}$$

where Z_{ij} is the worth acquired from the trial information and min (Z_{ij}) is the base of an incentive from the investigation. Correspondingly, max (Z_{ij}) is the most extreme worth obtained from the analysis for that specific reaction.

The subsequent step is to figure out grey relational coefficient for the standardized information utilizing the following equation.

$$GRC_{ij} = \frac{(\delta_{\min} + \gamma\delta_{\max})}{(\delta_{ij} + \gamma\delta_{\max})}, \tag{6}$$

where, $i = 1, 2, 3, \ldots, n$ and $j = 1, 2, 3, \ldots, m$.

GRC_{ij} is grey relational coefficients for the i_{th} explore/preliminary and j_{th} subordinate variable/reaction esteem. δ outright is unique among y_{oj} and y_{ij}, which is a distinction from the objective worth and can be treated as a quality misfortune. γ is the distinctive coeffective which is ordinarily fixed at 0.5.

The last step is to create a grey relational assessment for the test data. Besides, this is the most astonishing estimation of GRG which suggests the best parameters. The GRG is settled by using the equation as shown

$$GRG_{ij} = \frac{1}{n}\sum_{i=0}^{n} GRC_{ij}. \tag{7}$$

3. Results and Discussion

The response parameters such as MRR and Ra were analyzed through Taguchi single-objective optimization and ANOVA. The responses were converted into a regression equation to evaluate the optimized parameters from Taguchi analysis by using a multiobjective optimization technique called grey relational analysis (GRA). Table 4 demonstrates the attained MRR and Ra values with their respective signal-to-noise ratio. We then determined the S/N to maximize the MRR and minimize the Ra by larger the better and smaller the better

criteria. The optimal level for MRR and Ra was found by the mean S/N ratio.

3.1. Main Effect on MRR. Figure 5 depicts the effect of input parameters such as reinforcement wt. %, $p$on, $p$off, and WF in the response to MRR during WEDM of developed composites in Taguchi's analysis.

It is seen from Figure 5 that the expansion in weight level of fortifications to the base material fundamentally diminishes the MRR and the elements, for example, $p$on and WF at more elevated levels work on the MRR, while the expansion in $p$off adds to the lessening in MRR. The principle justification behind the reduction in MRR during machining is because of an expansion in hardness of the composites on the expansion of the support to a specific rate over the base material and furthermore because of the low electrical conductive nature of the essential support HNT.

The results from the previous experiment on WEDM regarding MRR decreased due to their hardness and electrical conductivity of the material, but the factor wire feed rate kept at a higher level the MRR increased, whereas the presence of larger particles in composites tends to decrease MRR by protecting the matrix material from melting [17, 18]. It is quite obvious that the increase in the wire feed rate from lower to higher level increases the spark energy verification and the material removal significantly causes an increase in MRR.

3.2. Main Effect on Ra. Figure 6 reveals that better surface roughness characteristics are obtained from factors such as the increase in poff and other factors. Pon, WF, and reinforcements are at lower levels.

The main factor to increase the surface roughness value is the addition of hard reinforcements over the base material, which makes the machining a complicated process in which the increase in poff reduces the spark supply over the wire causing a decrease in Ra. Both the reinforcements HNT and Zr in material base magnesium significantly cause a decrease in MRR and an increase in Ra during the WEDM process.

3.3. ANOVA. Table 5 shows the ANOVA results for MRR, it reveals that the weight percentage of HNT in magnesium MMC's majorly contributes to MRR in WEDM as 49% and Zr weight percentage contributes 15.48% and other factors Pon 17.576% and Poff 8.9% and WF 7.2% during the machining process. It can also be seen from Table 5 the % of contribution in various factors for determining the Ra, where the presence of reinforcements HNT and Zr contributes 46% and 20.2%, respectively, in determining the Ra of Magnesium MMCs. WF shows the least contribution as 2.5% and Pon contributes 13% to the Ra on machining of Magnesium MMC's and the main machining parameter P off shows a major contribution as 17.3% over that of another machining parameter in determining the Ra value.

Main Effects Plot for SN ratios
Material Removal Rate (MRR)
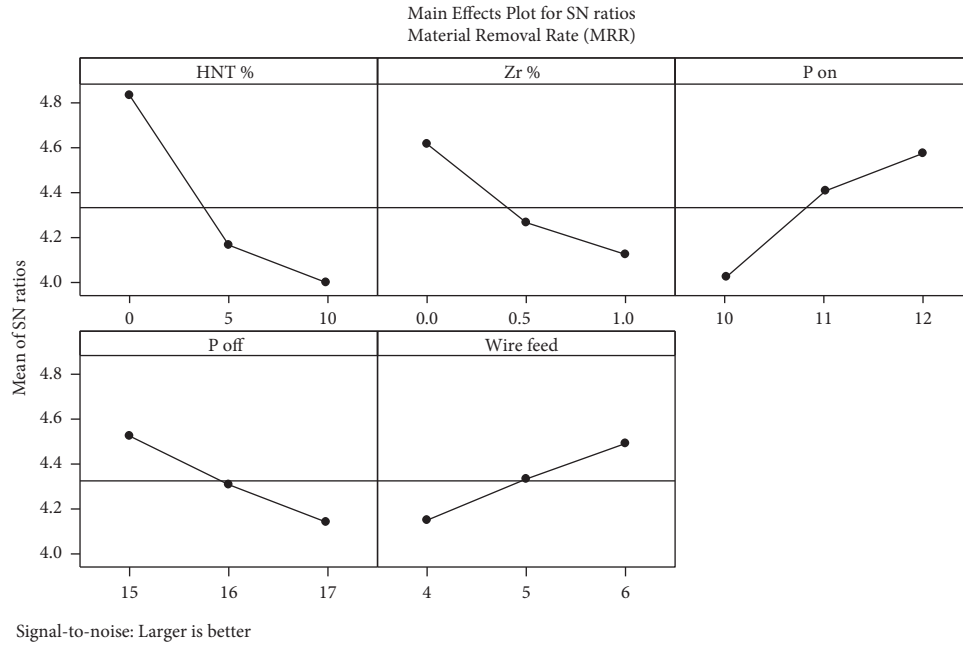
FIGURE 5: Result of input process parameters on MRR.

Main Effects Plot for SN ratios
Surface Roughness (Ra)
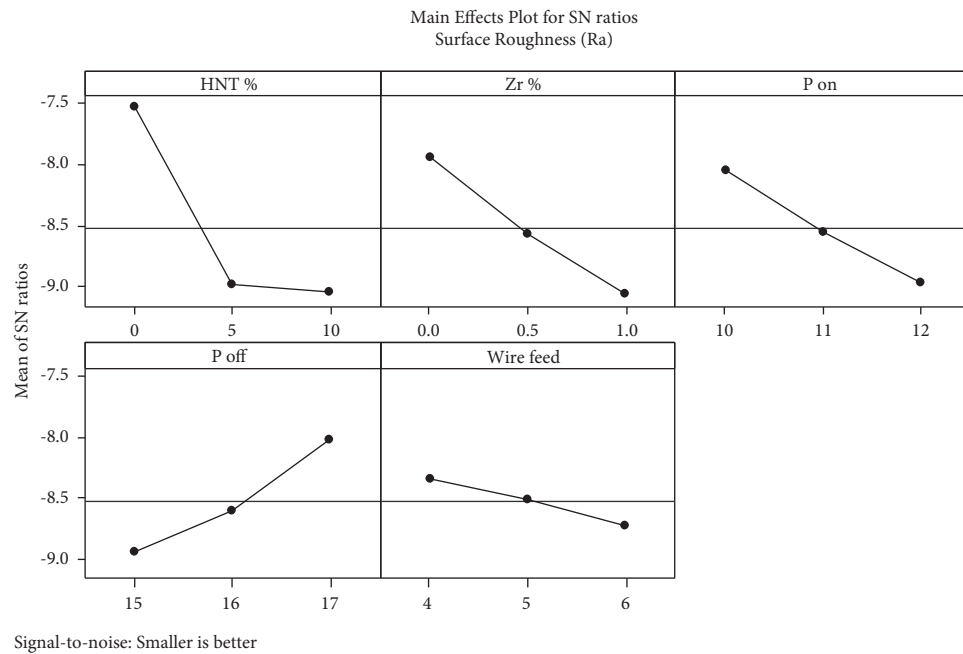
FIGURE 6: Result of input process parameters on Ra.

3.4. Mathematical Modeling. The regression equation has been formulated with the aid of the statistical software Minitab 16 to evaluate the optimized parameters from Taguchi's method and ANOVA. The regression equation for MRR and Ra is given as follows:

$$MRR = 1.64 - 0.0159 \times A - 0.0924 \times B + 0.0494 \times C \\ - 0.0357 \times D + 0.0323 \times E, \tag{8}$$

$$Ra = 3.00 + 0.0465 \times A + 0.346 \times B + 0.139 \times C \\ - 0.160 \times D + 0.0613 \times E. \tag{9}$$

TABLE 5: Analysis of variance for MRR and Ra.

Source of variance	DF	Sum of squares		Adjusted MS	F value	P-value	%C
		Sequential	Adjusted				
Material removal rate-MRR ($R^2 = 0.9808$, adj. $R^2 = 0.9687$)							
HNT %	2	0.127564	0.127564	0.063782	203.46	$p \leq 0.001$	48.956
Zr %	2	0.040353	0.040353	0.020177	64.36	$p \leq 0.001$	15.486
P on	2	0.045791	0.045791	0.022896	73.04	$p \leq 0.001$	17.576
P off	2	0.023055	0.023055	0.011527	36.77	$p \leq 0.001$	8.848
WF	2	0.018788	0.018788	0.009394	29.97	$p \leq 0.001$	7.210
Error	16	0.005016	0.005016	0.009394			
Total	26	0.260566					
Surface roughness-Ra ($R^2 = 0.9985$, adj. $R^2 = 0.9976$)							
HNT %	2	1.24545	1.24545	0.62272	2556.27	$p \leq 0.001$	46.670
Zr %	2	0.53957	0.53957	0.26978	1107.46	$p \leq 0.001$	20.219
P on	2	0.34900	0.34900	0.17450	716.32	$p \leq 0.001$	13.077
P off	2	0.46277	0.46277	0.23139	949.83	$p \leq 0.001$	17.341
WF	2	0.06794	0.06794	0.03397	139.44	$p \leq 0.001$	2.545
Error	16	0.00390	0.00390	0.00024			
Total	26	2.66862					
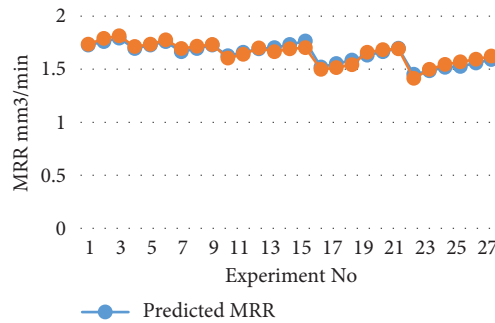
FIGURE 7: Actual Vs predicted MRR.
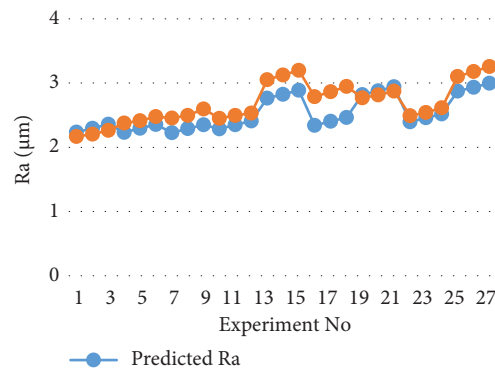
FIGURE 8: Actual Vs predicted Ra.

Figures 7 and 8 uncover the analysis results and their anticipated consequences of MRR and Ra values for the arrangement of preliminary courses of action. It is evident that trial and anticipated outcomes present a superior relationship with one another addressing an ostensible blunder deviancy among the exploratory and anticipated aftereffects of both MRR and Ra. From now, in light of Figures 7 and 8, it tends to be nitty gritty that equations (8) and (9) have a superior arrangement in determining the MRR and Ra values with the trial values, consequently used capably to expect the recently referenced output response inside the possibility of scattering.

3.5. Multiobjective Optimization

3.5.1. GRA. The GRA method was used to normalize the response parameters by "Smaller the better" and "Larger the

TABLE 6: Calculated GRG and its order in the optimization process.

Trial. No	Normalized values		Grey relational coefficient		Grey relational grade	Rank
	MRR	Ra	MRR	Ra		
1	0.800995	1	0.715302	1	0.857651	3
2	0.937811	0.967831	0.889381	0.939551	0.914466	2
3	1	0.911765	1	0.85	0.925	1
4	0.746269	0.806066	0.663366	0.72053	0.691948	6
5	0.803483	0.775735	0.717857	0.690355	0.704106	5
6	0.90796	0.715074	0.844538	0.637002	0.74077	4
7	0.70398	0.737132	0.628125	0.655422	0.641773	8
8	0.753731	0.698529	0.67	0.623853	0.646927	7
9	0.79602	0.605699	0.710247	0.559096	0.634671	9
10	0.475124	0.738971	0.487864	0.657005	0.572434	12
11	0.564677	0.69761	0.534574	0.623139	0.578857	11
12	0.711443	0.665441	0.634069	0.599119	0.616594	10
13	0.626866	0.186581	0.57265	0.380686	0.476668	21
14	0.691542	0.119485	0.618462	0.362184	0.490323	17
15	0.723881	0.054228	0.644231	0.345836	0.495033	16
16	0.21393	0.430147	0.388781	0.467354	0.428068	22
17	0.251244	0.357537	0.400398	0.437651	0.419025	24
18	0.323383	0.284007	0.424947	0.411187	0.418067	25
19	0.614428	0.44761	0.564607	0.475109	0.519858	15
20	0.676617	0.405331	0.607251	0.456759	0.532005	13
21	0.696517	0.351103	0.622291	0.4352	0.528746	14
22	0	0.704963	0.333333	0.628902	0.481118	20
23	0.21393	0.655331	0.388781	0.591948	0.490365	18
24	0.330846	0.591912	0.42766	0.550607	0.489133	19
25	0.38806	0.141544	0.449664	0.368065	0.408865	27
26	0.452736	0.071691	0.477435	0.350064	0.41375	26
27	0.524876	0	0.512755	0.333333	0.423044	23

TABLE 7: A typical response for GRG.

Level	HNT wt.%	Zr wt.%	Pulse on time	Pulse OFF time	Wire feed
1	0.7508	0.6717	0.6025	0.6005	0.5643
2	0.4763	0.5622	0.5723	0.5536	0.5766
3	0.4995	0.4927	0.5518	0.5724	0.5857
Delta	0.2745	0.1790	0.0508	0.0469	0.0214
Rank	1	2	3	4	5

better" and calculate the GRC as shown in Table 6. The GRG value was calculated by the average value of GRC concerning MRR and Ra. (0.5 weight was given for both MRR and RA). The parameter combination which has the highest value of GRG was considered as an optimum condition. The results attained from Taguchi coupled GRA were identical. From Table 6, it very well may be distinguished that the reinforcement wt. % increases when the MRR decreases and Ra increases. At lower p ON the Ra was decreased, and p ON and wire feed was high. Maximum MRR was reached at the machining of Mg MMC which strengthened with the base degree of reinforcements.

Table 7 shows the optimal conditions for better MRR and Ra values using the mean table or response table for GRG. According to the study, the parameter level which has the most elevated mean worth was considered as the optimal parameter level. For simple portrayals, optimum parameter levels are mentioned in bold figure in Table 7, and Figure 9 also graphically represents the effects of process parameters.

Table 8 shows the ANOVA results for GRG and it confirmed that each process parameter attained a significant effect over response parameters and it also revealed that the percentage of the weight of HNT has the maximum influence on GRG (70.561%) followed by Zr weight percentage

Main Effects Plot for Means
GRG
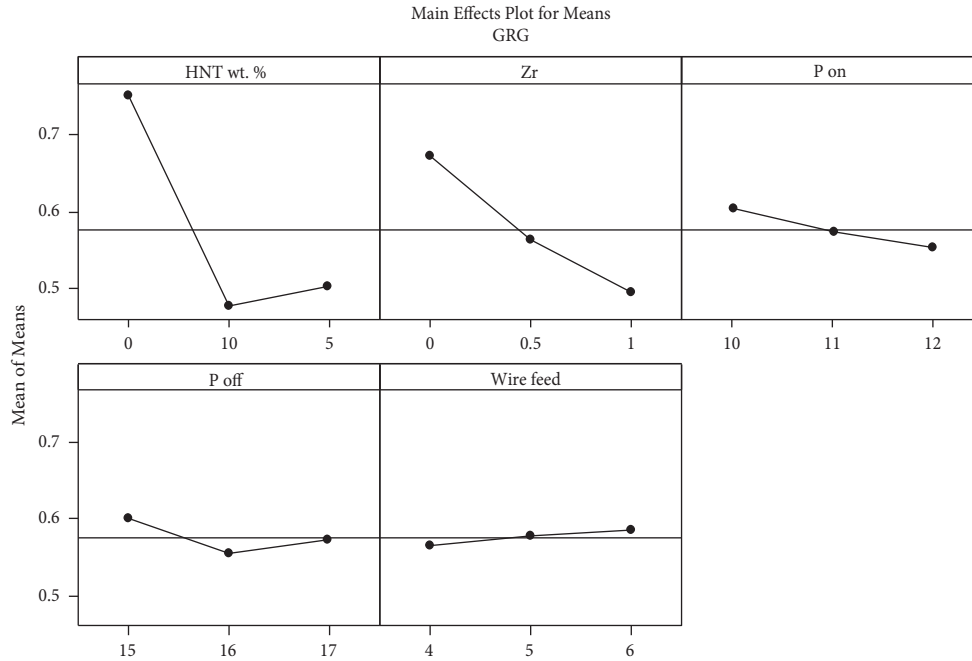
FIGURE 9: Main effects plot of the mean of means on GRG.

TABLE 8: Analysis of variance for GRG.

| Source of variance | DF | Sum of squares | | Adjusted MS | F value | P-value | % C |
		Sequential	Adjusted				
HNT %	2	0.417190	0.417190	0.208595	946.07	$p \leq 0.001$	70.561
Zr %	2	0.146672	0.146672	0.073336	332.61	$p \leq 0.001$	24.807
P on	2	0.011741	0.011741	0.005870	26.63	$p \leq 0.001$	1.985
P off	2	0.010033	0.010033	0.005016	22.75	$p \leq 0.001$	1.70
WF	2	0.002079	0.002079	0.001040	4.72	$p \leq 0.001$	0.351
Error	16	0.003528	0.003528	0.000220			0.596
Total	26	0.591242					100
		$R^2 = 0.994$, adj. $R^2 = 0.9903$					

(24.807%), Pulse ON time (1.98%), Pulse OFF time(1.20%), and wire feed (0.351%).

4. Conclusion

The WEDM studies were performed on the freshly evolved hybrid Mg-based MMCs and the accompanying conclusions were made.

(i) The addition of HNT and Zr into the Mg causes a small percentage increase in density because of the higher solidity of reinforcements.

(ii) An increase in hardness was accomplished by the addition of reinforcements with the Mg matrix.

(iii) Machinability of composite decreases as the Wt. % of reinforcements increases.

(iv) The optimal combination of input parameters identified by Taguchi-coupled GRA is lower level reinforcement percentage, pulse OFF time, pulse ON time, and higher-level wire feed rate.

(v) The developed regression equation predicts a nominal error deviancy among the predicted and experimental results of both Ra and MRR.

(vi) The optimal conditions recommended by GRA for attained higher MRR and lower Ra is revealed that the percentage of the weight of HNT has the greatest influence on GRG (70.561%), followed by Zr weight percentage (24.807%), pulse ON time (1.98%), pulse OFF time (1.20%), and wire feed (0.351%).

Data Availability

The data supporting the current study are given in the article.

Disclosure

The authors wish to declare and acknowledge that this article is available as a pre-print in Research Square and the same is cited in this study.

Conflicts of Interest

The authors declare that they have no conflicts of interest.

References

[1] R. Casati and M. Vedani, "Metal matrix composites reinforced by nano-particles—a review," *Metals*, vol. 4, no. 1, pp. 65–83, 2014.

[2] L. Dobrzanski and M. Adamiak, "Mechanically milled aluminium matrix composites reinforced with halloysite nanotubes," *Journal of Achievements in Materials and Manufacturing Engineering*, vol. 55, p. 654, 2012.

[3] A. Jayaganthan and K. S. Prakash, "Influence of machining parameters of electrochemical micromachining process over magnesium based hybrid metal matrix composite," *Materials Research Express*, vol. 6, no. 2, Article ID 026510, 2018.

[4] V. Kavimani and K. S. Prakash, "Tribological behaviour predictions of R-GO reinforced Mg composite using ANN coupled Taguchi approach," *Journal of Physics and Chemistry of Solids*, vol. 110, pp. 409–419, 2017.

[5] V. Kavimani, K. S. Prakash, M. S. Starvin, B. Kalidas, V. Viswamithran, and S. R. Arun, "Tribo-surface characteristics and wear behaviour of SiC @ r-GO/Mg composite worn under varying control factor," *Silicon*, vol. 12, 2019.

[6] L. Liu, X. Chen, F. Pan, S. Gao, and C. Zhao, "A new high-strength Mg-Zn-Ce-Y-Zr magnesium alloy," *Journal of Alloys and Compounds*, vol. 688, pp. 537–541, 2016.

[7] S. Mohanty, B. Routara, and R. Bhuayan, "Experimental investigation of machining characteristics for Al-SiC12% composite in electro-discharge machining," *Materials Today Proceedings*, vol. 4, no. 8, pp. 8778–8787, 2017.

[8] P. M. Gopal and K. S. Prakash, "Wire electric discharge machining of silica rich E-waste CRT and BN reinforced hybrid magnesium MMC," *Silicon*, vol. 11, no. 3, pp. 1429–1440, 2019.

[9] K. Ravindra, G. Manasi, G. Sheetal, and P. B. Kumar, "Halloysite nanotubes and applications: a review," *Journal of Advanced Scientific Research Available*, vol. 3, no. 2, pp. 25–29, 2012.

[10] A. Pramanik and G. Littlefair, "Wire EDM mechanism of MMCs with the variation of reinforced particle size," *Materials and Manufacturing Processes*, vol. 31, no. 13, pp. 1700–1708, 2016.

[11] A. Prasad, K. Siva, M. Tamil, and A. krishnaiah, "parametric optimization in wire electrical discharge machining of titanium alloy using response surface methodology," *Materials Today Proceedings*, vol. 4, no. 2, pp. 1434–1441, 2017.

[12] J. Singh, "Fabrication characteristics and tribological behavior of Al/SiC/gr hybrid aluminum matrix composites: a review," *Friction*, vol. 4, no. 3, pp. 191–207, 2016.

[13] K. P. Somashekhar, N. Ramachandran, and J. Mathew, "Material removal characteristics of micro slot (kerf) geometry in μ-WEDM on aluminum," *International Journal of Advanced Manufacturing Technology*, vol. 51, no. 5–8, pp. 611–626, 2010.

[14] J. Soyama, M. Oehring, W. Limberg, T. Ebel, K. U. Kainer, and F. Pyczak, "The effect of zirconium addition on sintering behaviour, microstructure and creep resistance of the powder metallurgy processed alloy Ti–45Al–5Nb–0.2B–0.2C," *Materials & Design*, vol. 84, pp. 87–94, 2015.

[15] D. Veerabrahmam, "Optimization of process parameters of wire-cut electric discharge machining of A356 . 2 aluminum alloy," *International Journal of Advanced Mechanical Engineering*, vol. 8, no. 1, pp. 173–180, 2018.

[16] K. Vetri Velmurgan and K. Venkatesan, "Experimental investigation and optimization of machining parameters using grey-relational analysis approach and fuzzy based Taguchi loss function method," *Indian Journal of Science and Technology*, vol. 9, no. 44, 2016.

[17] H. Zhang, Y. Zhao, Y. Yan et al., "Microstructure evolution and mechanical properties of Mg matrix composites reinforced with Al and Nano SiC particles using spark plasma sintering followed by hot extrusion," *Journal of Alloys and Compounds*, vol. 725, pp. 652–664, 2017.

[18] J. Anandan, K. S. Prakash, L. Jino, E. Manoj, A. Jacob, and S. A. Suthan, *Multi-objective optimization of WEDM parameters on Mg-HNT-Zr hybrid metal matrix composite using Taguchi coupled GRA*, Research Square Preprint, Durham, NC, USA, 2022.